SANDIA REPORT
SAND2019-9621

Printed September 2019

Sandia National Laboratories

The Thermalization Verification Problem for EMPIRE-PIC and EMPIRE-Fluid

Sidney Shields, Daniel S. Jensen, Brandon M. Medina, Troy C. Powell, Timothy D. Pointon, Chris H. Moore

Prepared by
Sandia National Laboratories
Albuquerque, New Mexico 87185
Livermore, California 94550

Issued by Sandia National Laboratories, operated for the United States Department of Energy by National Technology & Engineering Solutions of Sandia, LLC.

NOTICE: This report was prepared as an account of work sponsored by an agency of the United States Government. Neither the United States Government, nor any agency thereof, nor any of their employees, nor any of their contractors, subcontractors, or their employees, make any warranty, express or implied, or assume any legal liability or responsibility for the accuracy, completeness, or usefulness of any information, apparatus, product, or process disclosed, or represent that its use would not infringe privately owned rights. Reference herein to any specific commercial product, process, or service by trade name, trademark, manufacturer, or otherwise, does not necessarily constitute or imply its endorsement, recommendation, or favoring by the United States Government, any agency thereof, or any of their contractors or subcontractors. The views and opinions expressed herein do not necessarily state or reflect those of the United States Government, any agency thereof, or any of their contractors.

Printed in the United States of America. This report has been reproduced directly from the best available copy.

Available to DOE and DOE contractors from

U.S. Department of Energy
Office of Scientific and Technical Information
P.O. Box 62
Oak Ridge, TN 37831

Telephone: (865) 576-8401
Facsimile: (865) 576-5728
E-Mail: reports@osti.gov
Online ordering: http://www.osti.gov/scitech

Available to the public from

U.S. Department of Commerce
National Technical Information Service
5301 Shawnee Road
Alexandria, VA 22312

Telephone: (800) 553-6847
Facsimile: (703) 605-6900
E-Mail: orders@ntis.gov
Online order: https://classic.ntis.gov/help/order-methods

ABSTRACT

We report on the verification of elastic collisions in EMPIRE-PIC and EMPIRE-Fluid in support of the ATDM L2 V&V Milestone. The thermalization verification problem and the theory behind it is presented along with an analytic solution for the temperature of each species over time. The problem is run with both codes under multiple parameter regimes. The temperature over time is compared between the two codes and the theoretical results. A preliminary convergence analysis is performed on the results from EMPIRE-PIC and EMPIRE-Fluid showing the rate at which the codes converge to the analytic solution in time (EMPIRE-Fluid) and particles (EMPIRE-PIC).

CONTENTS

LIST OF FIGURES

LIST OF TABLES

1. INTRODUCTION

Modeling elastic collisions in the EMPIRE-PIC and EMPIRE-Fluid plasma codes is an important first step in improving the physics capabilities of these codes. While EMPIRE-PIC and EMPIRE-Fluid are both plasma codes, the models that they are based on operate under different assumptions and regimes. The parameters of the so-called thermalization problem were chosen so that both the fluid and kinetic descriptions of the gas are valid, such that the results of the two codes can be verified with each other, as well as an analytic solution.

The thermalization problem is a simple Zero-dimensional (0D) problem designed to specifically test and verify the elastic collision models in EMPIRE-PIC and EMPIRE-Fluid. The problem consists of two neutral species (to avoid electromagnetic effects) at two different temperatures that are expected to thermalize to the same equilibrium temperature through the effects of elastic collisions. To ensure that the thermalization is the result of only elastic collisions, the problem was kept spatially uniform with periodic boundary conditions.

Section 2 discusses the underlying models behind the two codes, the differences and similarities between them, and how elastic collisions are incorporated into these models. Section 3 then shows a comparison of the two codes and the analytic solution for the thermalization problem in several different parameter regimes. Finally, Section 4 shows a preliminary convergence analysis of the two codes to the analytic solution. Section 5 concludes the report.

2. THEORY

Elastic collisions are a special type of collision in which both momentum and energy are conserved. In this section we describe the theory used for modeling elastic collisions in both EMPIRE-Fluid and EMPIRE-PIC. We describe a general binary elastic collision, the Differential scattering Cross Section (DCS), and the Boltzmann equation. The basic theory introduced in this section is described in many texts such as Ref. [5] and is included here to define the notation used throughout this report. We derive the collision rate equations for EMPIRE-Fluid in Sec. 2.1 and describe the particle collision method for EMPIRE-PIC in Sec. 2.2.

An example of an elastic collision between two particles labeled α and β as viewed in the laboratory frame is given in Fig. 2-1. In the following discussion, all post-collision variables are primed, temperatures are written in energy units (e.g. T_α contains the Boltzmann factor), and formulas are written in SI units. The general formula for a binary collision between particle species α and β in which no new particles are created can be written as

$$\alpha\left(\mathbf{v}_\alpha\right)+\beta\left(\mathbf{v}_\beta\right)\rightarrow\alpha\left(\mathbf{v}'_\alpha\right)+\beta\left(\mathbf{v}'_\beta\right), \tag{1}$$

where $\mathbf{v}_\alpha$ and $\mathbf{v}_\beta$ are the particle velocities. The conservation of momentum equation

$$m_\alpha\mathbf{v}_\alpha+m_\beta\mathbf{v}_\beta=m_\alpha\mathbf{v}'_\alpha+m_\beta\mathbf{v}'_\beta \tag{2}$$

and conservation of energy equation

$$\frac{1}{2}m_\alpha v_\alpha^2 + \frac{1}{2}m_\beta v_\beta^2 = \frac{1}{2}m_\alpha \left(v'_\alpha\right)^2 + m_\beta \left(v'_\beta\right)^2 \tag{3}$$

determine the resulting particle velocities after the collision, where m_α and m_β are the particle masses. The Center of Mass (CM) velocity

$$\mathbf{G} = \frac{m_\alpha \mathbf{v}_\alpha + m_\beta \mathbf{v}_\beta}{m_\alpha + m_\beta}, \tag{4}$$

relative velocity

$$\mathbf{g} = \mathbf{v}_\alpha - \mathbf{v}_\beta, \tag{5}$$

and reduced mass

$$m_{\alpha\beta} = \frac{m_\alpha m_\beta}{M} \tag{6}$$

can be used to rewrite Eqs. (2)-(3) in the CM frame as

$$M\mathbf{V} = M\mathbf{V}' \tag{7}$$

and

$$\frac{1}{2}MV^2 + \frac{1}{2}m_{\alpha\beta}g^2 = \frac{1}{2}M\left(V'\right)^2 + \frac{1}{2}m_{\alpha\beta}\left(g'\right)^2, \tag{8}$$

where $M = m_\alpha + m_\beta$ is the total mass. Notice that the CM velocity remains constant during this collision because no external forces are present. The magnitude of the relative velocity is also constant, ($g = g'$), and only the direction is allowed to change during the collision as can be seen by combining Eqs. (7)-(8) and simplifying.

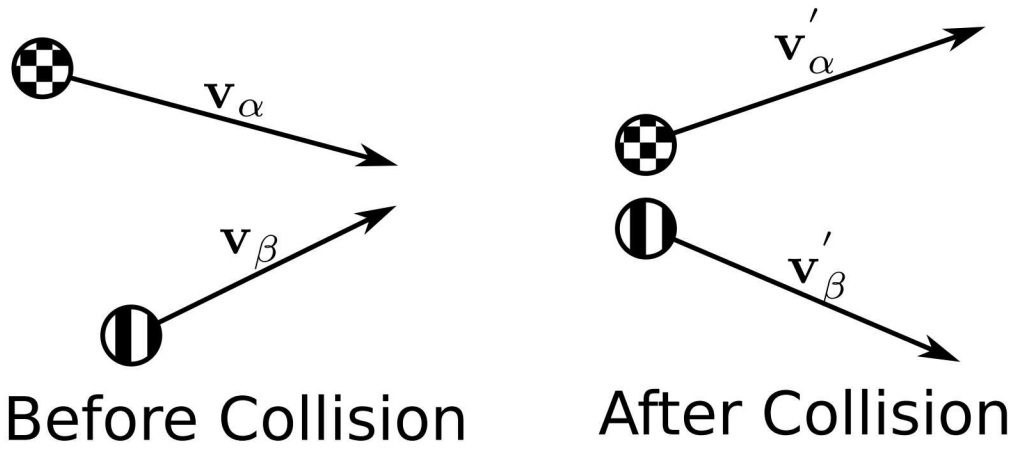

Figure 2-1 A binary elastic collision between two particles of species α and β illustrating the velocities of the particles before and after the collision.

The angular distribution of the post-collision velocities is determined by the DCS

$$\frac{\mathrm{d}\sigma}{\mathrm{d}\Omega} = \frac{(\text{number of scattered particles})\,/\,(\text{unit solid angle})\,/\,(\text{unit time})}{(\text{number of target particles})\cdot[(\text{number of incident particles})\,/\,(\text{unit time})\,/\,(\text{unit area})]}. \tag{9}$$

Without loss of generality, let's assume that a particle of type β is the target particle at rest for a beam of particles of type α directed along the positive z axis. Then the DCS in the CM frame is written as $\frac{\mathrm{d}\sigma}{\mathrm{d}\Omega}(g,\Omega)$, where Ω is the solid angle between the initial and final relative velocities. Assuming that the differential cross section does not depend on the azimuthal angle, the momentum transfer is given by

$$\int \mathrm{d}\Omega \left(\mathbf{g}-\mathbf{g}'\right) \frac{\mathrm{d}\sigma}{\mathrm{d}\Omega}(g,\chi) = -\mathbf{g}\sigma^{\mathrm{tr}}(g) \tag{10}$$

where the momentum transfer cross section is defined by

$$\sigma^{\mathrm{tr}} = 2\pi \int_0^{\pi} \sin\chi \mathrm{d}\chi \, (1-\cos\chi) \frac{\mathrm{d}\sigma}{\mathrm{d}\Omega}(g,\chi), \tag{11}$$

and χ is the polar angle illustrated in Fig. 2-2. The DCS will be used in the Boltzmann equation described below to model the collision rates in both EMPIRE-Fluid and EMPIRE-PIC.

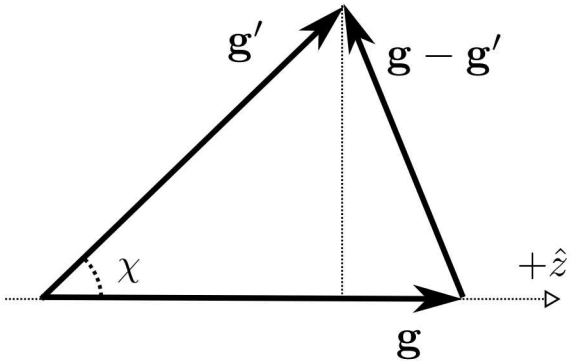

Figure 2-2 The relative velocity vectors and corresponding polar angle χ.

The Boltzmann equation for a system of particles of type α with a one-particle distribution function $f_\alpha(\mathbf{x},\mathbf{v},t)$ is [2]

$$\frac{\partial f_\alpha}{\partial t} + \mathbf{v}\cdot\nabla_{\mathbf{x}} f_\alpha + \frac{q_\alpha}{m_\alpha}(\mathbf{E}+\mathbf{v}\times\mathbf{B})\cdot\nabla_{\mathbf{v}} f_\alpha = \left(\frac{\delta f_\alpha}{\delta t}\right)^c, \tag{12}$$

where the collision term for elastic collisions is

$$\left(\frac{\delta f_\alpha}{\delta t}\right)^c = \int \mathrm{d}\mathbf{v}_\beta \int \mathrm{d}\Omega \left[f_\alpha(\mathbf{v}'_\alpha) f_\beta(\mathbf{v}'_\beta) - f_\alpha(\mathbf{v}_\alpha) f_\beta(\mathbf{v}_\beta)\right] g \frac{\mathrm{d}\sigma}{\mathrm{d}\Omega}(g,\chi) \tag{13}$$

The fluid density is

$$n_\alpha(\mathbf{x},t) = \int \mathrm{d}\mathbf{v} \, f_\alpha(\mathbf{x},\mathbf{v},t), \tag{14}$$

the fluid velocity is

$$\mathbf{u}_\alpha(\mathbf{x},t) = \frac{1}{n_\alpha}\int \mathrm{d}\mathbf{v}\,\mathbf{v} f_\alpha(\mathbf{x},\mathbf{v},t), \tag{15}$$

and the fluid temperature is

$$\mathbf{T}_\alpha(\mathbf{x},t) = \frac{\gamma-1}{n_\alpha}\int \mathrm{d}\mathbf{v}\,\frac{1}{2} m_\alpha (\mathbf{v}-\mathbf{u}_\alpha)^2 f_\alpha(\mathbf{x},\mathbf{v},t), \tag{16}$$

where γ is the species' adiabatic index, (e.g. $\gamma = 5/3$ for a monatomic gas). The distribution function for a given species α is assumed to be close to a local drifting Maxwellian distribution

$$f_\alpha(\mathbf{x},\mathbf{v},t) = \left(\frac{m_\alpha}{2\pi T_\alpha(\mathbf{x},t)}\right)^{3/2} n_\alpha(\mathbf{x},t)\exp\left(-\frac{m_\alpha(\mathbf{v}-\mathbf{u}_\alpha(\mathbf{x},t))^2}{2T_\alpha(\mathbf{x},t)}\right) \tag{17}$$

Taking moments of Eq. (13) gives us

$$\frac{\partial n_\alpha}{\partial t} + \nabla\cdot(n_\alpha u_\alpha) = \dot{n}_\alpha^c, \tag{18a}$$

$$\frac{\partial \mathbf{p}_\alpha}{\partial t} + \nabla\cdot\left(\mathbf{p}_\alpha\mathbf{u}_\alpha^T\right) = -\nabla\cdot\underline{\mathrm{P}}_\alpha + q_\alpha n_\alpha(\mathbf{E}+\mathbf{u}_\alpha\times\mathbf{B}) + \dot{\mathbf{p}}_\alpha^c, \text{ and} \tag{18b}$$

$$\frac{\partial w_\alpha}{\partial t} + \nabla\cdot(w_\alpha\mathbf{u}_\alpha) = -\nabla\cdot\mathbf{q}_\alpha - \nabla\cdot(\underline{\mathrm{P}}_\alpha\cdot\mathbf{u}_\alpha) + q_\alpha n_\alpha\mathbf{E}\cdot\mathbf{u}_\alpha + \dot{w}_\alpha^c, \tag{18c}$$

where $\mathbf{p}_\alpha = n_\alpha m_\alpha\mathbf{u}_\alpha$ is the momentum density, $w_\alpha = \frac{1}{\gamma-1}n_\alpha T_\alpha + \frac{1}{2}n_\alpha m_\alpha u_\alpha^2$ is the total kinetic energy density,

$$\underline{\mathrm{P}}_\alpha = m_\alpha\int \mathrm{d}\mathbf{v}\,(\mathbf{v}-\mathbf{u}_\alpha)(\mathbf{v}-\mathbf{u}_\alpha)^T f_\alpha(\mathbf{x},\mathbf{v},t) \tag{19}$$

is the pressure tensor and

$$\mathbf{q}_\alpha = \frac{m_\alpha}{2}\int \mathrm{d}\mathbf{v}\,(\mathbf{v}-\mathbf{u}_\alpha)(\mathbf{v}-\mathbf{u}_\alpha)^2 f_\alpha(\mathbf{x},\mathbf{v},t) \tag{20}$$

is the heat flux vector. The c superscript stands for the collision terms resulting from taking moments with the collision operator. We now introduce the scalar pressure $p_\alpha = n_\alpha T_\alpha$ and scalar stress tensor $\underline{\Pi}_\alpha = \underline{\mathrm{P}}_\alpha - p_\alpha\underline{\mathrm{I}}$, where $\underline{\mathrm{I}}_{ij} = \delta_{ij}$ is the unit tensor. We assume the distribution function is spherically symmetric so that the stress tensor is zero. In this case we can rewrite the momentum equation, Eq. (18b), as

$$\frac{\partial \mathbf{p}_\alpha}{\partial t} + \nabla\cdot\left(\mathbf{p}_\alpha\mathbf{u}_\alpha^T\right) = -\nabla p_\alpha + q_\alpha n_\alpha(\mathbf{E}+\mathbf{u}_\alpha\times\mathbf{B}) - \nabla\cdot\underline{\Pi}_\alpha + \dot{\mathbf{p}}_\alpha^c \tag{21}$$

and the temperature equation, Eq. (18c), as

$$\frac{\partial}{\partial t}\left(\frac{1}{\gamma-1}n_\alpha T_\alpha\right) + \nabla\cdot\left(\frac{1}{\gamma-1}n_\alpha T_\alpha\right)\mathbf{u}_\alpha = -n_\alpha T_\alpha\nabla\cdot\mathbf{u}_\alpha - \nabla\cdot\mathbf{q}_\alpha - \underline{\Pi}_\alpha\nabla\mathbf{u}_\alpha + \frac{1}{\gamma-1}n_\alpha\dot{T}_\alpha^c \tag{22}$$

2.1. Fluid Collisions

In order to derive the fluid collision rates, we need to take velocity moments of the elastic collision operator given in Eq. (13)

$$\frac{\partial\Psi^c}{\partial t} = \int \mathrm{d}\mathbf{v}_\alpha\int \mathrm{d}\mathbf{v}_\beta\, f_\alpha f_\beta g\int \mathrm{d}\Omega\,\frac{\mathrm{d}\sigma}{\mathrm{d}\Omega}(g,\chi)\left(\psi'-\psi\right), \tag{23}$$

where $\psi = 1$ for the density equation, $\psi = m_\alpha \mathbf{v}_\alpha$ for the momentum equation, and $\psi = m_\alpha \left(\mathbf{v}_\alpha - \mathbf{u}_\alpha\right)^2/2$ for the temperature equation. The $(\psi' - \psi)$ terms can be rewritten in terms of the variables $\mathbf{G}$ and $\mathbf{g}$ producing the expressions

$$m_\alpha \left(\mathbf{v}'_\alpha - \mathbf{v}_\alpha\right) = -m_\beta \left(\mathbf{v}'_\beta - \mathbf{v}_\beta\right) = m_{\alpha\beta} \left(\mathbf{g}' - \mathbf{g}\right) \tag{24}$$

for the momentum equation and the expressions

$$\psi'_\alpha - \psi_\alpha = m_\alpha \left[\left(\mathbf{v}'_\alpha - \mathbf{u}_\alpha\right)^2 - \left(\mathbf{v}'_\alpha - \mathbf{u}_\alpha\right)^2\right]/2 = m_{\alpha\beta} \left(\mathbf{G} - \mathbf{u}_\alpha\right) \cdot \left(\mathbf{g}' - \mathbf{g}\right) \tag{25a}$$

$$\psi'_\beta - \psi_\beta = m_\beta \left[\left(\mathbf{v}'_\beta - \mathbf{u}_\beta\right)^2 - \left(\mathbf{v}'_\beta - \mathbf{u}_\beta\right)^2\right]/2 = -m_{\alpha\beta} \left(\mathbf{G} - \mathbf{u}_\beta\right) \cdot \left(\mathbf{g}' - \mathbf{g}\right) \tag{25b}$$

for the temperature equation.

The integrations in Eq. (23) for the momentum and temperature equations are carried out in App. A. The final collision rates (corresponding to the collision terms of Eqs. (21)-(22)) for two fluids with elastic collisions are

$$\dot{\mathbf{p}}^c_\alpha = -\nu_{\alpha\beta} m_{\alpha\beta} n_\alpha \left(\mathbf{u}_\alpha - \mathbf{u}_\beta\right), \tag{26a}$$

$$\dot{\mathbf{p}}^c_\beta = -\nu_{\beta\alpha} m_{\alpha\beta} n_\beta \left(\mathbf{u}_\beta - \mathbf{u}_\alpha\right), \tag{26b}$$

$$\dot{T}^c_\alpha = (\gamma - 1)\left[-\nu^E_{\alpha\beta}\left(T_\alpha - T_\beta\right) + \frac{m_\beta}{T_\beta}\left(\frac{m_\alpha}{T_\alpha} + \frac{m_\beta}{T_\beta}\right)^{-1} \nu_{\alpha\beta} m_{\alpha\beta} U^2_{\alpha\beta}\right], \tag{26c}$$

$$\dot{T}^c_\beta = (\gamma - 1)\left[-\nu^E_{\beta\alpha}\left(T_\alpha - T_\beta\right) + \frac{m_\alpha}{T_\alpha}\left(\frac{m_\alpha}{T_\alpha} + \frac{m_\beta}{T_\beta}\right)^{-1} \nu_{\beta\alpha} m_{\alpha\beta} U^2_{\alpha\beta}\right], \tag{26d}$$

where the momentum transfer collision frequency is

$$\nu_{\alpha\beta} = n_\beta \Sigma^{\mathrm{tr}}_{13}\left(v_{\alpha\beta}, U_{\alpha\beta}\right) \tag{27}$$

and the temperature equilibration collision frequency is

$$\nu^E_{\alpha\beta} = \frac{m_{\alpha\beta}}{m_\alpha + m_\beta} n_\beta \Sigma^{\mathrm{tr}}_{05}\left(v_{\alpha\beta}, U_{\alpha\beta}\right). \tag{28}$$

The $\Sigma^{\mathrm{tr}}_{13}$ and $\Sigma^{\mathrm{tr}}_{05}$ terms are given by the formulas

$$\Sigma_{0n}\left(v_{\alpha\beta}, U_{\alpha\beta}\right) = \frac{v_{\alpha\beta}}{\sqrt{2\pi}} \int_0^\infty dw\, w^n e^{-\frac{1}{2}(w-z)^2} S_0(wz)\, \sigma\left(w v_{\alpha\beta}\right) \text{ and}$$

$$\Sigma_{1n}\left(v_{\alpha\beta}, U_{\alpha\beta}\right) = \frac{v_{\alpha\beta}}{\sqrt{2\pi}} \int_0^\infty dw\, w^n e^{-\frac{1}{2}(w-z)^2} \left(\frac{w}{z}\right) S_1(wz)\, \sigma\left(w v_{\alpha\beta}\right),$$

where $w = g/v_{\alpha\beta}$, $z = U_{\alpha\beta}/v_{\alpha\beta}$, $U_{\alpha\beta} = \mathbf{u}_\alpha - \mathbf{u}_\beta$, and $v_{\alpha\beta} = \sqrt{T_\alpha/m_\alpha + T_\beta/m_\beta}$. The S_m functions are given by the formula

$$S_m(x) = e^{-x} \int_{-1}^{1} \mathrm{d}y\, y^m e^{xy} \tag{29}$$

with

$$S_0(x) = \frac{2e^{-x}\sinh x}{x} \text{ and} \tag{30a}$$

$$S_1(x) = 2e^{-x}\left(\frac{\cosh x}{x} - \frac{\sinh x}{x^2}\right). \tag{30b}$$

The rate equations given above also agree with the results of Ref. [4] in which the rates for a general excitation collision simplify to those of an elastic collision when the absorption energy is zero.

2.2. Particle Collisions

EMPIRE-PIC uses Sandia Particle INteraction (SPIN) to compute particle-particle (and soon fluid-particle) collisions. SPIN implements the Direct Simulation Monte Carlo (DSMC) method [1], which simulates the evolution of the velocity distribution of a fluid by computing stochastic collisions between a relatively small number of representative particles (at most millions or billions instead of the huge numbers involved in physical systems). Each time step, each computational cell determines how many pairs of particles it will test for interactions based on the local density of particles and the cross sections of each specific interaction (e.g., a Helium-Helium elastic collision, or an electron-Argon ionization). Then the method samples pairs and finds the probability that a pair collides by comparing the relative likelihood that the pair collides against a reference value.

For this problem, we used a very simple model – our molecules are Maxwell molecules (i.e. molecules with an artificially selected cross section of $\sigma(g) = \sigma_0/g$), and they undergo only elastic collisions with isotropic scattering. The distinguishing feature of Maxwell molecules is that the likelihood of a collision between two molecules is independent of their relative speed so that for a given interaction all pairs are equally likely to collide. Isotropic elastic collisions involve only a uniform random scattering of a pair's relative velocity vector, conserving momentum and energy. SPIN can simulate more complicated physics like ionization, but the additional logic for this should make no difference to this test.

3. VERIFICATION

3.1. Simple Case: 0 drift velocity, equal densities, and equal species

The first case used was the simple case of two particle/fluid species, with velocities $\mathbf{v}_\alpha = \mathbf{v}_\beta = 0$ m/s (velocity is taken to be bulk velocity in the case of EMPIRE-PIC), densities $n_\alpha = n_\beta = 1 \times 10^{25}\ \#\cdot\mathrm{m}^{-3}$, and initial temperatures $T_\alpha(0) = 1000$ K, $T_\beta(0) = 100$ K. Both species' masses and charges were set to that of neutral helium, $m_\alpha = m_\beta = 6.6464764 \times 10^{-27}$

kg. The parameters chosen here allow us to simplify Eq. 26 to a system of linear Ordinary Differential Equations (ODEs). This solution can be expressed in closed form:

$$T_\alpha = 550 + 450e^{-\frac{4}{3}\nu_{\alpha\beta}t} \tag{31a}$$

$$T_\beta = 550 - 450e^{-\frac{4}{3}\nu_{\alpha\beta}t} \tag{31b}$$

Here, $\nu_{\alpha\beta} = \frac{m_{\alpha\beta}}{m_\alpha + m_\beta} 3 n_\beta \sigma_0$, where σ_0 is the reference cross section.

For the sake of mathematical simplicity while calculating the analytic solution, both species were assumed to have Maxwell molecule cross sections as explained in section 2. The reference cross section used in this Maxwell molecule model was $\sigma_0 = 1 \times 10^{-18}\,\mathrm{m}^2$. While these cross sections are not based on realistic data, they allow us to verify the underlying elastic collisions model by giving us an analytic solution to compare to.

One assumption that the analytic solution and EMPIRE-Fluid's underlying model makes about each of its individual fluids is that each one will stay thermalized within its own species. In other words, at any point of the domain it can be assumed that a specific fluid has a definable temperature, and that all of the particles' velocities that that fluid represents are in a Maxwellian distribution. As it is not necessarily the case that physically the two species' distributions remain in equilibrium while equilibrating with one another (it depends on the cross sections velocity dependence), we force EMPIRE-PIC's species to remain in equilibrium by setting the particle-particle collision rate within a single species to be 100 times larger than the inter-species collision rate. The fluctuating error seen in EMPIRE-PIC's results are mainly a result of using a finite number of computational particles in the simulation. As can be seen in 4, increasing the number of particles decreases this fluctuation in error.

The simulation was run in both codes on a $[-1 \times 10^{-5}, 1 \times 10^{-5}] \times [-1 \times 10^{-5}, 1 \times 10^{-5}]\ \mathrm{m}^2$ domain with periodic boundary conditions, and was discretized with a 4×4 rectangular mesh. The initial conditions were then chosen to be spatially constant to make the problem effectively 0D in space. The simulation was run with a time-step of $dt = .1$ ns, and a final time of $T_f = 200$ ns. The EMPIRE-PIC simulations were run with 15000 particles per species.

To compare the effects of the collisions across codes, the temperature of each fluid/particle species was measured at each time step. Figure 3-1 shows a comparison plot of EMPIRE-PIC, EMPIRE-Fluid, and the analytic solution over all time in the solution. Figure 3-2 shows the error of both codes over all time, which shows fairly good agreement between the two codes and the analytic solution at all timesteps.

3.2. Electron Beam Case: large drift velocity, different densities, and different species

To showcase the accuracy of these elastic collision models in a more realistic scenario, we created a test case of an electron beam traveling through a background gas. Electron beams traveling

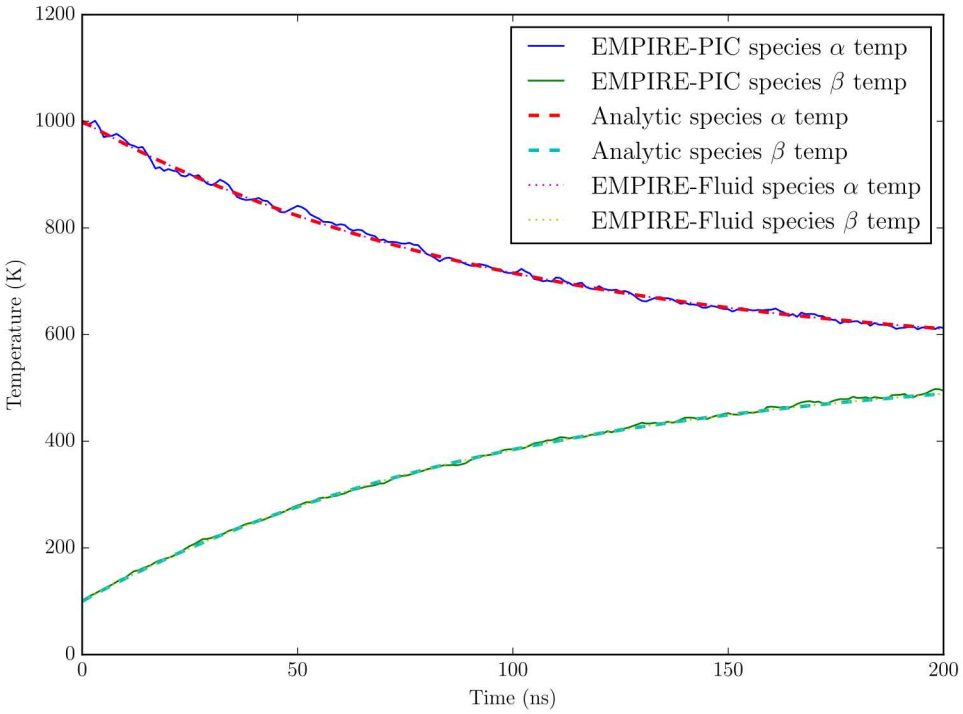

Figure 3-1 Plot comparing the particle/fluid temperatures for EMPIRE-PIC, EMPIRE-Fluid, and the analytic solution.

through a background gas occur in many different plasma applications, and in many cases the effects of elastic collisions between the beam and the gas is significant enough that it needs to be accounted for. To emulate an electron beam traveling through a background gas, the following parameters were chosen: $\mathbf{v}_\alpha = 8.4 \times 10^7\,\hat{\mathbf{x}}$ m/s, $\mathbf{v}_\beta = 0$ m/s, $n_\alpha = 1 \times 10^{24}\,\#\cdot\mathrm{m}^{-3}$, $n_\beta = 1 \times 10^{25}\,\#\cdot\mathrm{m}^{-3}$, $T_\alpha(0) = 1000$ K, $T_\beta(0) = 100$ K, $m_\alpha = 9.1093836 \times 10^{-31}$ kg, $m_\beta = 6.6464764 \times 10^{-27}$ kg. Here β was chosen to represent the electron species and α was chosen to represent the background gas (helium in this case).

The simulation was run in both codes on a $[-1,1] \times [-1,1]$ m^2 domain with periodic boundary conditions and was discretized with 4×4 rectangular mesh. The initial conditions were then chosen to be spatially constant to make the problem effectively 0D in space. The simulation was run with a time-step of $dt = .1$ ns and a final time of $T_f = 500$ ns. The EMPIRE-PIC simulations were run with 4×10^4 particles for species α and 4×10^5 particles for species β to keep the particle weights the same across species.

The analytic solution in this case does not simplify to a system of linear ODEs, so we do not have a closed form for it. The ODEs that represent the analytic solution in this case were solved using an ODE solver from Python's SciPy library [3]. Solver tolerances were tuned such that the solver error was negligible compared to the error from EMPIRE-PIC and EMPIRE-Fluid, and therefore was not a factor in the shown error plots and convergence analysis. In Figure 3-3 and 3-4 we can once again see good agreement between the two codes and the analytic solution.

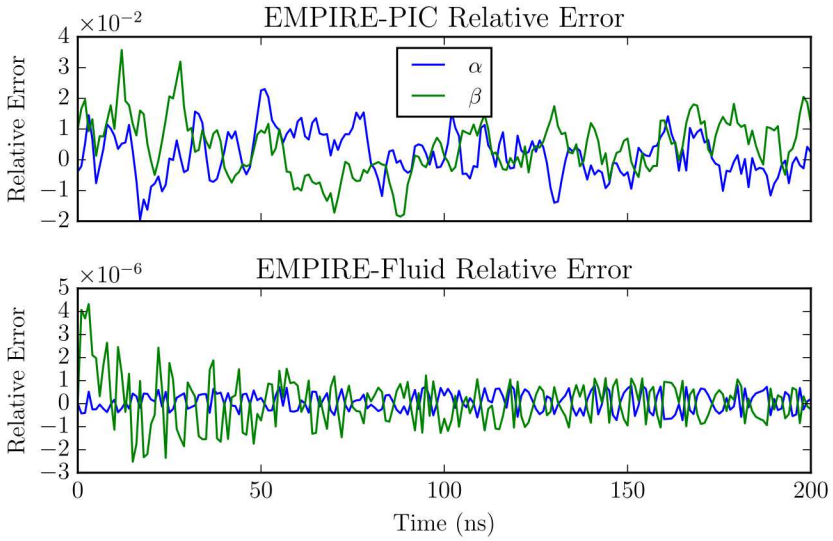

Figure 3-2 Error plots for the temperatures of both species. Top: EMPIRE-PIC, Bottom: EMPIRE-Fluid.

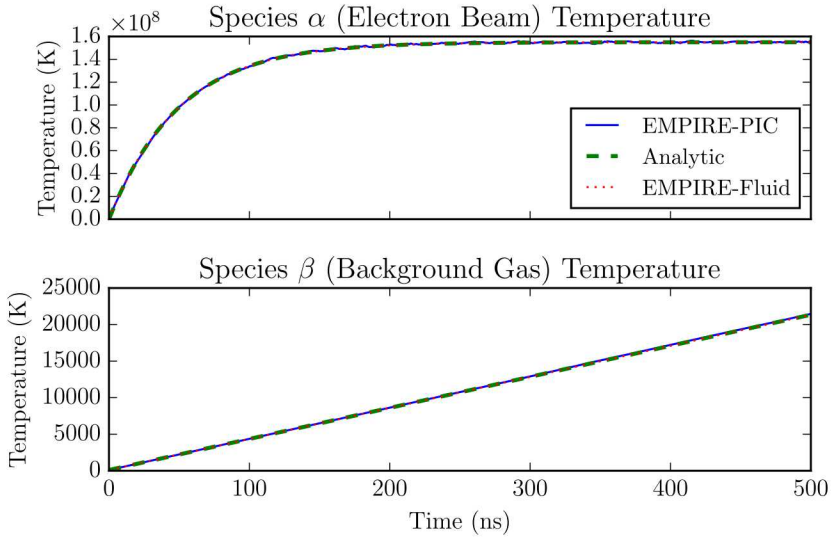

Figure 3-3 Plots comparing temperatures for EMPIRE-PIC, EMPIRE-Fluid, and the analytic solution. Top: Electron beam temperatures, Bottom: Helium background gas temperatures.

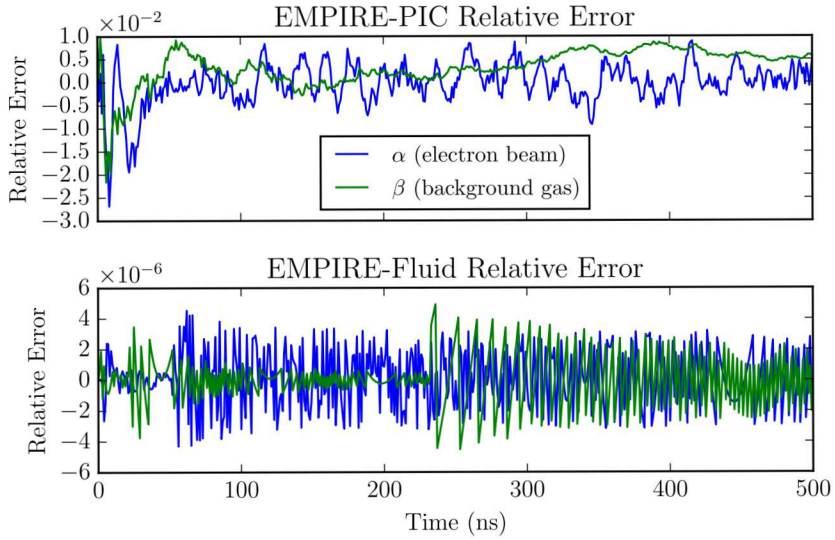

Figure 3-4 Error plots for the temperatures of both species. Top: EMPIRE-PIC, Bottom: EMPIRE-Fluid.

4. CONVERGENCE

4.1. EMPIRE-PIC Convergence

As an initial convergence analysis for EMPIRE-PIC, convergence in particles was tested using the simple case from Sec. 3. Spatial convergence was not tested for this problem, because it is a 0D problem. To test convergence in particle count for EMPIRE-PIC with this problem, the problem was run for various particle counts ranging from $N_p = 5$ particles per cell to $N_p = 160$ particles per cell. The temperature at $t = 50$ ns was then measured in the simulation and compared to the analytic solution at that time.

Because EMPIRE-PIC is a stochastic code using a Monte Carlo method to compute the collisions (the DSMC method), each simulation seed using the same parameters produces a different result, and therefore a different error. To account for this, a large number of simulations were run for each particle count, from which the mean and standard deviation of the relative error was calculated.

The number of simulations run for each particle count started at 10^4 simulations for $N_p = 5$ particles per cell and then decreased by a factor of $\sqrt{2}$ each time the number of particles was doubled in order to keep the variance of the error constant with varying N_p. These mean relative errors (with 2 standard deviation error bars) are plotted below in Figure 4-1 on top of the plot of the expected order of convergence for this algorithm. These results show good agreement with the expected order of convergence of N_p^{-1}.

Timestep convergence was not tested here because the error signal due to the time-solver is much less than the noise introduced by even large numbers (10^5) of computational particles. It, however, will be examined in the future in a more rigorous manner using StREEQ.[6]

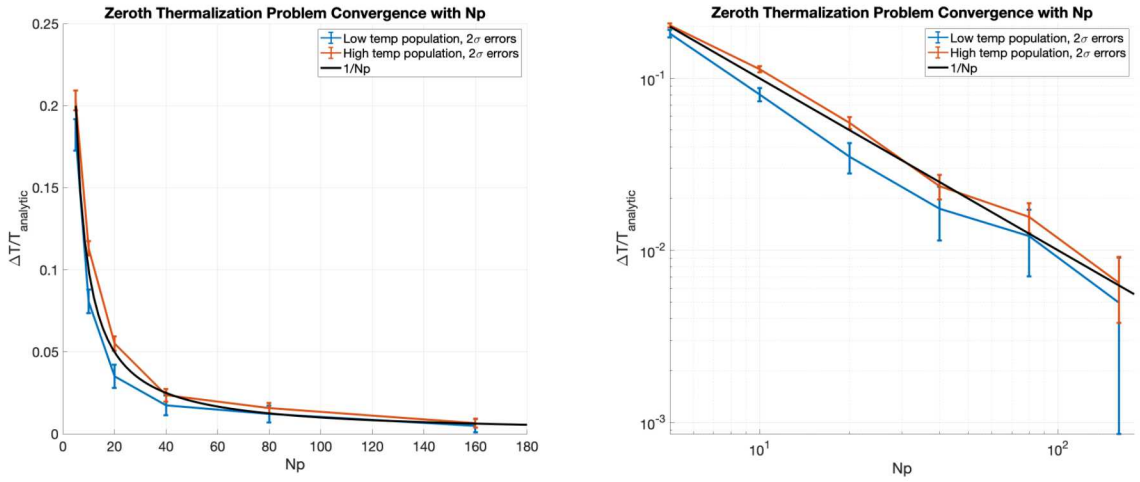

Figure 4-1 Left: Convergence plot of the relative mean errors compared to the expected convergence of N_p^{-1}. Right: Log-log plot of the convergence plot.

4.2. EMPIRE-Fluid Convergence

As in EMPIRE-PIC's case, spatial convergence was not shown in this problem for EMPIRE-Fluid because this is a 0D problem. To test convergence in time for EMPIRE-Fluid, 5 different simulations were run with decreasing time-steps. The error for each refinement was measured using the following L^2 norm in time for the space-averaged temperature over the entire domain:

$$||\text{avg}(T_h) - T||_{L^2} = \sqrt{\int_0^{T_f} (\text{avg}(T_h(t)) - T(t))^2 dt}, \tag{32}$$

where T is the analytic temperature, T_h is the computed temperature, and T_f is the final time of the simulation.

The problem was set up the same as the simple case in Section 3, but for varying timesteps. The timestepping algorithm used was Third-order Strong Stability Preserving Runge-Kutta (SSPRK3), with an expected order of convergence of $\mathcal{O}(dt^3)$. The following table and plot of errors show very good agreement with the expected order of convergence and the observed order of convergence.

Table 4-1 Table showing convergence rates of the L^2 error between time refinements.

dt	L^2 Error	Convergence Rate
4.00E-08	0.000444498085782	–
2.00E-08	4.82642427351243E-05	3.203150557796
1.00E-08	5.57976587944494E-06	3.11267824862117
5.00E-09	6.58547455319421E-07	3.0828452787018
2.50E-09	1.02726218212021E-07	2.68048296641442

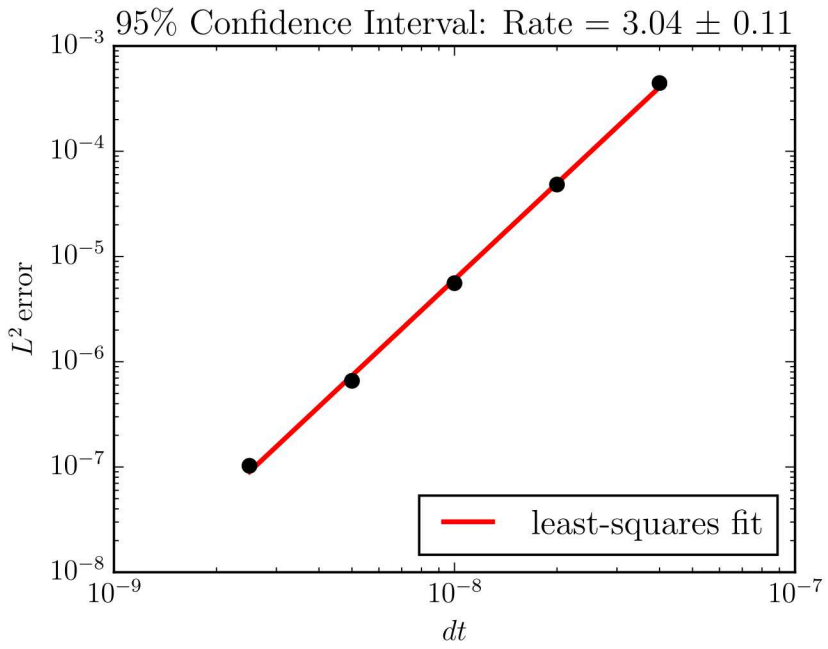

Figure 4-2 Convergence plot showing 3rd order convergence in time.

5. CONCLUSION

Both EMPIRE-PIC and EMPIRE-Fluid's elastic collision models show great agreement to the analytic solution for the chosen thermalization test problem. In addition, observed convergence results for EMPIRE-PIC was the expected N_p^{-1} in number of particles, and the observed converged results for EMPIRE-Fluid was the expected dt^3 in time. As such, we have increased our confidence that both EMPIRE-PIC and EMPIRE-Fluid model elastic collisions correctly as expected.

One limitation of the current EMPIRE-Fluid collision model shown in this report is the lack of ability to perform inelastic collisions. As a next step for this collision model, we plan to add ionization and excitation/de-excitation collisions to EMPIRE-Fluid. In addition, we plan to extend the elastic collisions in this report to EMPIRE-Hybrid, to allow collisional coupling between EMPIRE-Fluid and EMPIRE-PIC. Once added, the EMPIRE-Hybrid results should show strong agreement with the results presented here.

REFERENCES

[1] Graeme A Bird and JM Brady. Molecular gas dynamics and the direct simulation of gas flows, volume 5. Clarendon press Oxford, 1994.

[2] J. A. Bittencourt. Fundamentals of plasma physics. pages 506–508, 1995.

[3] Eric Jones, Travis Oliphant, Pearu Peterson, et al. SciPy: Open source scientific tools for Python (Version 1.2.1).

[4] Hai P. Le and Jean-Luc Cambier. Modeling of inelastic collisions in a multifluid plasma: Excitation and deexcitation. Physics of Plasmas, 22(9):093512, September 2015.

[5] M. Mitchner and Charles H. Kruger. Partially ionized gases. Wiley, New York, 1st edition edition, 1973.

[6] Gregg A. Radtke, Keith L. Cartwright, and Lawrence C. Musson. Stochastic Richardson extrapolation based numerical error estimation with application to kinetic plasma simulations. Technical report SAND2017-4165, Sandia National Laboratories, Albuquerque, New Mexico 87185 and Livermore, California 94550, 2017.

APPENDIX A.

We evaluate the velocity moments of the elastic collision operator, Eq. (23), by expressing the exponential terms in the Maxwellian distributions f_α and f_β in terms of the CM and relative velocities $\mathbf{G}$ and $\mathbf{g}$. The expressions are symmetric in α and β if we work in the reference frame traveling at $\mathbf{V} = \left(\mathbf{u}_\alpha + \mathbf{u}_\beta\right)/2$ such that $\mathbf{u}_\alpha = \mathbf{U}/2$ and $\mathbf{u}_\beta = -\mathbf{U}/2$, where $\mathbf{U} = \mathbf{u}_\alpha - \mathbf{u}_\beta$. We introduce the following variables as well to simplify the expressions:

$$A = \frac{1}{2}\left(\frac{m_\alpha}{T_\alpha} + \frac{m_\beta}{T_\beta}\right), \tag{33}$$

$$B = \frac{m_{\alpha\beta}}{2T_{\alpha\beta}}, \tag{34}$$

$$C = \frac{m_{\alpha\beta}}{m_\alpha + m_\beta}\frac{\left(T_\beta - T_\alpha\right)}{T_{\alpha\beta}}, \text{ and} \tag{35}$$

$$D = \frac{1}{2}\left(\frac{m_\alpha}{T_\alpha} - \frac{m_\beta}{T_\beta}\right)\left(\frac{m_\alpha}{T_\alpha} + \frac{m_\beta}{T_\beta}\right)^{-1}, \tag{36}$$

where the binary temperature is

$$T_{\alpha\beta} = m_{\alpha\beta}\left(\frac{T_\alpha}{m_\alpha} + \frac{T_\beta}{m_\beta}\right). \tag{37}$$

In order to normalize velocities it is helpful to define the binary thermal velocity

$$v_{\alpha\beta} = \sqrt{\frac{T_{\alpha\beta}}{m_{\alpha\beta}}} = \left(\frac{T_\alpha}{m_\alpha} + \frac{T_\beta}{m_\beta}\right)^{1/2}. \tag{38}$$

With the above definitions, we make the change of variable

$$\mathbf{H} = \mathbf{G} + C\mathbf{g} - D\mathbf{U} \tag{39}$$

in Eq. (23) to obtain

$$\frac{\partial \Psi^c}{\partial t} = n_\alpha n_\beta \left(\frac{AB}{\pi^2}\right)^{3/2} \int \mathrm{d}\mathbf{H}\, e^{-AH^2} \int \mathrm{d}\mathbf{g}\, g e^{-B(\mathbf{g}-\mathbf{U})^2} \int \mathrm{d}\Omega \frac{\mathrm{d}\sigma}{\mathrm{d}\Omega}(g,\chi)\left(\psi' - \psi\right). \tag{40}$$

Substituting Eq. (24) into Eq. (40) for the momentum transfer, the integral over Ω becomes the definition of the momentum transfer cross section, Eq. (11), while the integral over $\mathbf{H}$ is elementary. The resulting equation is

$$\dot{\mathbf{p}}_\alpha^c = -m_{\alpha\beta} n_\alpha n_\beta \left(\frac{B}{\pi}\right)^{3/2} \int \mathrm{d}\mathbf{g}\, g e^{-B(\mathbf{g}-\mathbf{U})^2} \mathbf{g}\sigma^{\mathrm{tr}}(g). \tag{41}$$

Likewise, substituting Eq. 25a into Eq. 40, replacing $\mathbf{G}$ with $\mathbf{H}$, and performing the elementary $\mathbf{H}$ integral gives the temperature change

$$\frac{1}{\gamma - 1} n_\alpha \dot{T}_\alpha^c = -m_{\alpha\beta} n_\alpha n_\beta \left(\frac{B}{\pi}\right)^{3/2} \int \mathrm{d}\mathbf{g}\, g e^{-B(\mathbf{g}-\mathbf{U})^2} \left[-Cg^2 + \left(D - \frac{1}{2}\right)\mathbf{g}\cdot\mathbf{U}\right]\sigma^{\mathrm{tr}}(g). \tag{42}$$

Equations (41)-(42) can be written as linear combinations of the S_0 and S_1 integrals defined in Eq. (30) and produce the final fluid collision rates given in Eq. (26).

Sandia National Laboratories is a multimission laboratory managed and operated by National Technology & Engineering Solutions of Sandia LLC, a wholly owned subsidiary of Honeywell International Inc., for the U.S. Department of Energy's National Nuclear Security Administration under contract DE-NA0003525.